Separation Science and Technology
Publication details, including instructions for authors and subscription information:
http://www.informaworld.com/smpp/title~content=t713708471

Selective Particle Deposition in Crossflow Filtration

Wei-Ming Lu[a]; Shang-Chung Ju[a]
[a] DEPARTMENT OF CHEMICAL ENGINEERING, NATIONAL TAIWAN UNIVERSITY TAIPEI, TAIWAN, REPUBLIC OF CHINA

To cite this Article Lu, Wei-Ming and Ju, Shang-Chung(1989) 'Selective Particle Deposition in Crossflow Filtration', Separation Science and Technology, 24: 7, 517 — 540
To link to this Article: DOI: 10.1080/01496398908049789
URL: http://dx.doi.org/10.1080/01496398908049789

SEPARATION SCIENCE AND TECHNOLOGY, 24(7 & 8), pp. 517-540, 1989

Selective Particle Deposition in Crossflow Filtration

WEI-MING LU* and SHANG-CHUNG JU

DEPARTMENT OF CHEMICAL ENGINEERING
NATIONAL TAIWAN UNIVERSITY
TAIPEI, TAIWAN, REPUBLIC OF CHINA

Abstract

To study the mechanism of particle deposition in crossflow filtration, hydrodynamic forces exerted on a spherical particle touching the surface of filter medium are analyzed to derive the critical selective cut-diameter of the deposited particles under various crossflow velocities and filtration rates in a crossflow filtration system. Experimental data of turbulent crossflow filtration of dilute light calcium carbonate suspension agree with the prediction of this theory within 30% error under the crossflow velocity of from 0.57 to 1.14 m/s. Equations to estimate the characteristics of crossflow filtration, such as steady-state filtration rate and average specific resistance of cake, are also presented.

INTRODUCTION

Crossflow filtration refers to the mode of operation which keeps the motion of a fluid parallel to the filter medium to limit further particle deposits on cake. Having the advantages of thin-cake, high filtration flux and continuous operation, this mode of filtration has become an effective and economical operation for obtaining a clear fluid from a suspension containing colloidal or submicro-sized particles. Similar to the concentration polarization effect in ultrafiltration, the suspension particles will be deposited on the filter septum and eventually result in resistance to filtration. Most researchers (*1-4*) have acknowledged that crossflow velocity is the key control variable in the deposition of cake as well as the filtration flux. Their experimental data showed that a higher crossflow

*To whom correspondence should be addressed.

velocity always induces a thinner cake and, as a result, gives a higher filtration rate, though a contradictory effect of filtration rate on crossflow velocity was observed (*5*). However, the mechanism of particle deposition in crossflow filtration is not well understood theoretically. In order to understand the effect of crossflow on filtration performance, it is essential to analyze how the crossflow influences the deposition mechanism of particles on the filter septum.

Recently, Zydney and Colton (*6*) modified the concept of concentration polarization and pointed out that satisfactory agreement with the polarization model could be obtained if shear-enhanced diffusivity of larger particles replaced the Brownian diffusivity of particles. However, this model assumed a very high concentration of particles at the wall, which was not observed in crossflow filtration. Davis and Leighton (*7*), in correcting the concentration effect on the shear-induced diffusivity of particles, proposed a similar model except for a nonlinear velocity profile within a sheared particle layer, and derived a criterion to predict the conditions needed to form a stagnant particle layer on the porous septum. However, neither quantitative data to support their theory nor the crossflow effect on the particle deposition and the filtration flux was presented.

Another theoretical approach is a purely hydrodynamic consideration which discards Fick's law to explain the migration of particles. By observing the shear-sweeping phenomenon of particles on a surface of a particulate packed bed, Shirato et al. (*8*) and Rushton et al. (*9*) investigated the crossflow effect on cake formation experimentally. Taking the lateral migration of a particle into account, various investigators (*10*, *11*) have shown that steady-state filtration flux can be attained as the filtration rate decays until it is equal to the lift velocity of a particle. However, a detailed calculation of lift velocity of a particle in a crossflow filtration system shows that it is always smaller than the filtration flux.

Lu et al. (*12*) analyzed the particle size distribution of different layers of cake formed from a rotary filter press and found that finer particles appeared in the upper layer of the cake. Fischer and Raasch (*5*) measured the particle size distribution in a cake formed under various crossflow velocities and found that most of the particles deposited on the cake came from finer parts of the initial slurry particles and that the higher crossflow velocity formed a finer particles cake. Furthermore, they (*13*) suggested that a critical selective cut-diameter of the deposited particles existed. By analyzing the forces exerted on a single spherical particle, Fischer and Raasch proposed a qualitative model to describe the selective cut-diameter of the deposited particle in crossflow filtration. Without any

theoretical derivation, they claimed that the tangent drag force due to crossflow velocity is proportional to the shear stress at the wall, τ_w, and the normal pressure force due to permeation flow is proportional to the filtration flux, q. And they then found that the critical selective cut-diameter of the deposited particle is proportional to q/τ_w, which explains why higher crossflow velocity forms a finer particle cake in crossflow filtration. However, their model cannot show the precise value of the cut-diameter of a deposited particle as well as the existence of the cut-diameter in crossflow filtration.

Obviously, for a turbulent crossflow filtration system, the lift force due to the inertial gradient of crossflow velocity will have some order of importance in particle deposition. In this paper, all the hydrodynamic forces acting on a deposited sphere are analyzed and then the concept of sediment transport is applied to derive a relationship between the largest selective cut-diameter of the deposited particles and other filtration variables. The existence of cut-diameter is checked by the measurement of particle size distribution in a cake and is found to compare with theory under various crossflow velocities. Finally the hydrodynamic theory is extended to describe the mechanism of particle deposition during crossflow filtration to yield a better understanding of the shearing effect on crossflow filtration.

THEORETICAL DEVELOPMENT

Velocity Field around the Deposited Particle

To develop a hydrodynamic model to describe the structure of particle deposition on the filter medium in a crossflow filtration system, one may start by determining how fluid flows around a particle on the surface of the filter medium. Since the diameter of the deposited particle is small compared with the thickness of the boundary layer existing on the surface, the analysis of flow around the particle can be limited to the velocity field within the boundary layer. The flow can be summarized as 1) tangential flow of fluid parallel to the septum, 2) fluid flow normal to the filter septum, and 3) permeation flow of fluid through the filter septum. Each of them can be simply described as follows.

I. Tangential Flow of Fluid Parallel to the Septum

The crossflow velocity very near the porous medium was obtained by Hirata and Ito (*14*) as

$$u^+ = \frac{\exp(-m_w^+ z^+) - 1}{m_w^+} + \frac{p^+}{(m_w^+)^2}[\exp(-m_w^+ z^+) + 1 - m_w^+ z^+] \quad (1)$$

where m_w^+ is the dimensionless suction mass velocity defined by Hirata and Ito. Since the values of m_w^+ and $m_w^+ z^+$ are far smaller than 1 in crossflow filtration, by expanding the exponential term in the Taylor series and analyzing the order of magnitude of each expanded term on the right-hand side of Eq. (1), it can be reduced to

$$u^+ = z^+ \quad (2)$$

or in a dimensional form

$$u = (u^{*2}/\nu)z = (u_m/\delta)z \quad (3)$$

which is similar to the expression of u^+ in an ordinary laminar sublayer without suction.

II. Fluid Flows Normal to the Filter Septum

Schlichting (*15*) and Hirata and Ito (*14*) showed that it is reasonable to assume a uniform suction velocity profile within the boundary layer or laminar sublayer to analyze the hydrodynamic behavior of external boundary-layer flow and internal pipe flow with wall suction. Therefore, one may assume that the undisturbed velocity in the normal direction is uniform through the sublayer in crossflow filtration, i.e.,

$$v = q \quad (4)$$

III. Permeation Flow of Fluid through the Filter Septum

By assuming an incompressible septum, uniform superficial velocity through the filter septum can be estimated by Darcy's law as

$$q = \Delta P/\mu R_m \quad (5)$$

where ΔP is the pressure drop between the filter septum and R_m is the resistance of the septum.

Drags Analysis

From the assumption as described in the previous section, the flow behavior of fluid within the laminar sublayer when a particle deposits on the porous septum can be simplified as shown in Fig. 1a. By solving the equations of continuity and motion in the case of very slow motion for the system shown in Fig. 1a, the overall drag acting on the particle can be obtained. Since the governing equations of creeping flow and the boundary conditions are all linear, the system can be separated into two independent solvable flow systems as shown in Fig. 1b. System 1 concerns a fluid with a linear-tangential velocity profile flowing over a sphere which stays on an impermeable wall, and System 2 concerns a fluid flowing uniformly and vertically over a sphere staying on a permeable wall and permeating through the septum. By solving the velocity distribution of fluid within these two systems independently, the

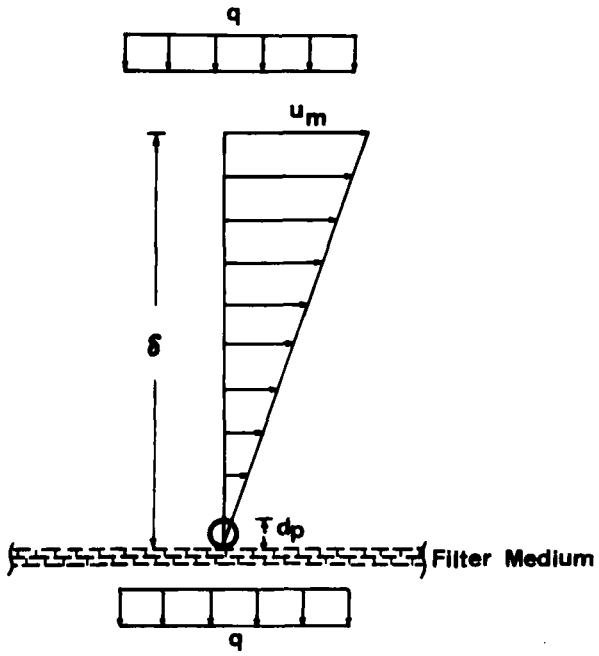

FIG. 1a. Simplified flow patterns of fluid around a spherical particle touching the surface of the filter in crossflow filtration.

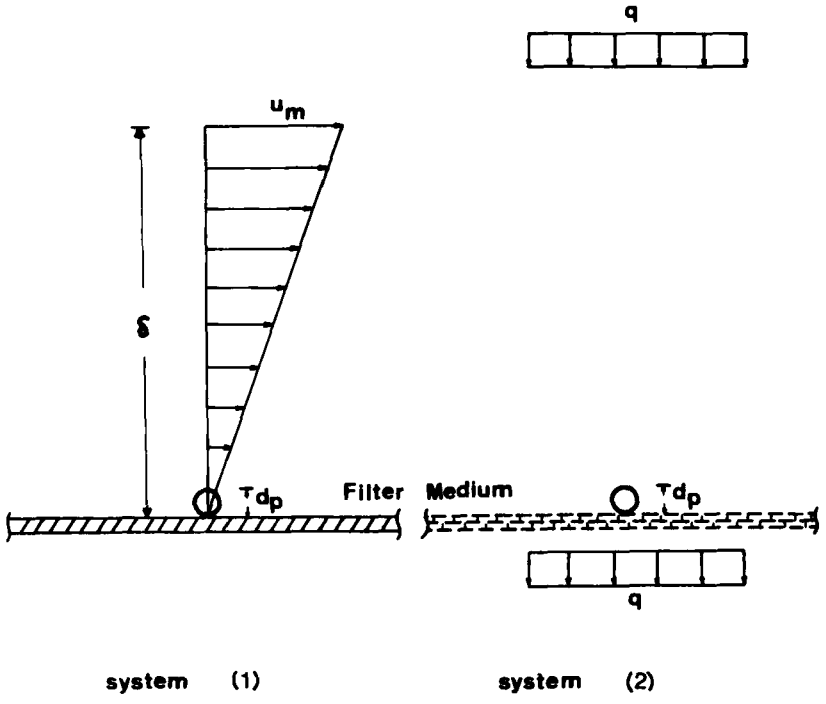

FIG. 1b. Two independent flow systems separated from the system shown in Fig. 1a.

drag exerted on the sphere can be obtained by integrating the stresses on the sphere and combining them.

For System 1, O'Neill (*16*) solved the drag force exerted on a single spherical particle touching an impermeable wall within a simple shear flow field and has given the drag as

$$F_t = 1.7009\{3\pi\mu d_p u_p(z = d_p/2)\} \tag{6}$$

where $u_p(z = d_p/2)$ is the undisturbed velocity at the position $z = d_p/2$, d_p is the diameter of the sphere, and 1.7009 is the wall correction factor of Stokes' law derived by O'Neill for this flow system.

Similar to System 2, Goren (*17*) solved the resisting drag of a sphere with uniform velocity U_∞ approaching a permeable wall, and he concluded that for a finite value of wall permeability a finite hydrodynamic force on the sphere was expected even for the sphere "touching" the wall. When the particle and wall were in contact, he derived the drag force as:

$$F = \phi 3\pi\mu d_p U_\infty \tag{7}$$

where ϕ is the wall correction factor of Stokes' law for the corresponding flow system. It can be estimated by

$$\phi = \left\{\frac{R_m d_p}{3} + (1.072)^2\right\}^{1/2} \tag{8}$$

Comparing it with our System 2, the permeation drag supporting a sphere remaining on the filter septum can be obtained by replacing U_∞ with the filtration rate q in Eq. (7), i.e.,

$$F_f = \phi 3\pi\mu d_p q \tag{9}$$

Lateral Lift Force

A theoretical analysis of the lateral migration velocity of a sphere within a simple shear flow field was derived by Saffman (*18*) for an unbounded fluid, and it was modified by Vasseur and Cox (*19*) for the case of Couette and Poiseuille bounded flow. For a neutrally buoyant spherical particle within Couette flow, the lift velocity of the sphere very near the bounded wall is

$$v_l = \frac{61}{576\nu}\left(\frac{u_m}{\delta}\right)^2\left(\frac{d_p}{2}\right)^3 \tag{10}$$

By combining this velocity with the filtration velocity of the fluid, Eq. (9) can be modified to give a net vertical drag on the sphere:

$$F_n = \phi 3\pi\mu d_p(q - v_l) \tag{11}$$

Finally, the rest force is the submerged weight force of the spherical particle which can be expressed by

$$F_w = \pi/6(\rho_p - \rho_s)g d_p^3 \tag{12}$$

Critical Cut-Diameter of Deposited Particles

Fluid flowing over a bed of sediment exerts forces on the grain, and these forces tend to move or entrain the particles. However, when the drag

force is less than some critical value, the bed material remains unmoved. A critical state is reached only when the forces acting on the particle bed are balanced or in equilibrium (*20*). Referring to Fig. 1c, the moment of all hydrodynamic forces about the contact point G can be calculated as as

$$M = d_p/2\{F_t \cos\theta - (F_n + F_w) \sin\theta\} \tag{13}$$

where θ is the angle of repose of the submerged particle and F_t, F_n, and F_w are hydrodynamic forces exerted on a particle which can be expressed by Eqs. (6), (11), and (12), respectively. The sign of the net moment calculated from Eq. (13) will determine whether or not the sphere will stay on the filter medium. A negative value of the net moment shows that the sphere will remain stable on the filter surface, and a positive value shows that the particle on the septum will be swept off the surface. When the net moment is equal zero, Eq. (13) can be rewritten as

$$F_t = (F_n + F_w) \tan\theta \tag{14}$$

By introducing Eqs. (6), (11), and (12) into Eq. (14) and rearranging the results, one obtains

$$q = \frac{1.7}{\phi \tan\theta} u_p(z = d_{pc}/2) - \frac{(\rho_p - \rho_s)}{18\mu\phi} g d_{pc}^2 + \frac{61}{576\nu}\left(\frac{u_m}{\delta}\right)^2\left(\frac{d_{pc}}{2}\right)^3 \tag{15}$$

where d_{pc} is the corresponding largest critical cut-diameter of deposited particles in crossflow filtration. Substituting Eq. (3) and the definition of $u^* = u_s\sqrt{f/2}$ into Eq. (15) leads to

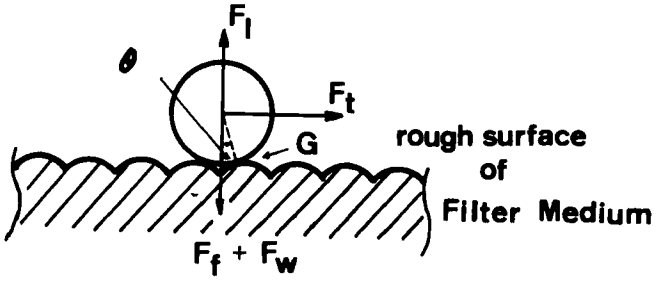

FIG. 1c. Hydrodynamic forces exerted on the spherical particle with an angle of repose θ between particle and filtering wall.

$$q = \frac{0.425 f u_s^2}{\phi \nu \tan\theta} d_{pc} - \frac{(\rho_p - \rho_s)}{18\mu\phi} g d_{pc}^2 + \frac{15.25 f^2 u_s^4}{4608\nu^3} d_{pc}^3 \qquad (16)$$

where f is the fanning friction factor and u_s is the average slurry velocity. The analysis of Mizushina et al. (*21*) showed very little effect of wall suction on the friction factor in the case of a crossflow filtration system. By using Dean's (*22*) correlations for rectangular duct flow with a high aspect ratio for the Reynold's number from 6.0×10^3 to 6.0×10^5, $f = 0.073\mathrm{Re}^{-1/4}$, Eq. (16) can be rewritten as

$$q = c_1 u_s^{7/4} d_{pc} - c_2 d_{pc}^2 + c_3 u_s^{7/2} d_{pc}^3 \qquad (17)$$

where

$$c_1 = \frac{0.02609}{\phi \tan\theta\, \nu^{3/4} H^{1/4}}$$

$$c_2 = \frac{(\rho_p - \rho_s) g}{18\mu\phi}$$

and

$$c_3 = \frac{1.247 \times 10^{-5}}{\nu^{5/2} H^{1/2}} \qquad (18)$$

By substituting the relationship between the friction factor and Reynold's number in the laminar flow region, $f = 24/\mathrm{Re}$, into Eq. (16) and neglecting the terms of inertial lift force, the selective cut-diameter of a deposited particle in the case of laminar crossflow filtration can also be derived as

$$q = c_4 u_s d_{pc} - c_2 d_{pc}^2 \qquad (19)$$

where

$$c_4 = \frac{5.1}{\phi \tan\theta\, H} \qquad (20)$$

Another corresponding formula in transitional crossflow filtration can also be derived if the f-Re correlation is known in the transitional flow region.

Equations (17) and (19) show the relationship between the selective critical cut-diameter of a deposited particle and filtration variables such as crossflow velocity and filtration rate in turbulent and laminar crossflow filtration, respectively. For a given crossflow velocity and filtration rate, the cut-diameters calculated by Eqs. (17) or (19) mean that if the diameters of the deposited particles are larger than the calculated cut-value, those particles may not remain stable on the cake surface. Only the particles whose diameters are smaller than the cut-diameter may deposit on the filter septum to form a cake.

Probability Function of Particle Deposition

Intuitively, particles of any size in a slurry have almost the same chance to approach the filter medium. In practical operation, particles whose diameters are larger than the critical value may have less chance to deposit on the filter surface. In order to describe the chance of deposition of a particle on the septum, a population balance of deposited particles can be taken for the particle diameter d_p on a thin layer of cake, i.e.,

$$\begin{pmatrix}\text{mass of particles with diameter } d_p \\ \text{stay on a differential layer of cake}\end{pmatrix} = \begin{pmatrix}\text{corresponding mass} \\ \text{of particles in} \\ \text{slurry carried by} \\ \text{filtrate flux}\end{pmatrix} \times \begin{pmatrix}\text{mass fraction of} \\ \text{particles with} \\ \text{diameter } d_p \text{ in} \\ \text{slurry}\end{pmatrix} \times \begin{pmatrix}\text{probability of par-} \\ \text{ticle deposition} \\ \text{with diameter } d_p\end{pmatrix}$$

Expressed in mathematic form:

$$f_c(d_p)dd_p\Delta w_c = \{c_0\Delta V\}\{f_0(d_p)dd_p\}\{P(d_p)\} \tag{21}$$

where $f_0(d_p)$ and $f_c(d_p)$ are the frequency functions of particle size distribution (mass base) of the initial slurry and the cake, respectively, and $P(d_p)$ is the probability function of particle deposition (which is always less than 1). Rearranging Eq. (21), one may express the probability function of particle deposition $P(d_p)$ in terms of the frequency function of initial slurry and cake as

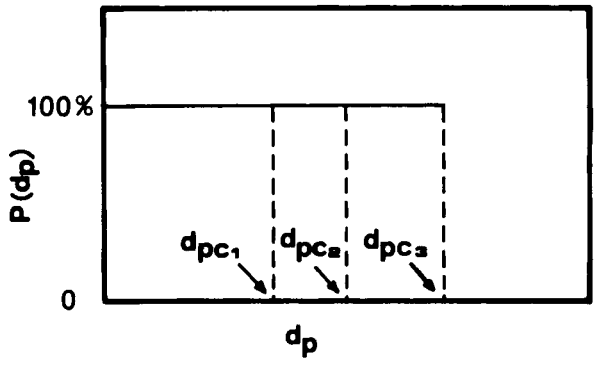

FIG. 2. Probability function of particle deposition when the crossflow selective effect is ideal.

$$P(d_p) = f_c(d_p)\Delta w_c / f_0(d_p) c_0 \Delta V \tag{22}$$

If the selective effect on crossflow filtration is ideal, then the probability function curve of particle deposition should be shown to be clear cut as in Fig. 2. All particles whose diameters are less than the critical value d_{pci} are deposited, and the rest will be swept away from the cake surface.

EXPERIMENTAL APPARATUS AND METHODS

Figure 3a shows the systematic diagram of a two-dimensional rectangular crossflow filter. Two parallel plates 1.44 m long and 5 cm wide, with a clearance of 0.7 cm, are assembled to construct the filter chamber. At a distance of 36.5 cm from the inlet, eight filtration septums, each having a filtration area of 5×10 cm^2, were installed in series on the lower side of plate. The detailed structure of the filter septum is shown in Fig. 3b. However, in this study the filter medium was installed only in the first section.

A 0.5 wt% dilute light calcium carbonate slurry was prepared, poured into a reservoir tank, and kept in suspension. A circulating pump was installed to move the flowing slurry parallel to the filter septum and to conduct the filtration. Clear filtrate was received by a vacuum receiver which was connected to a load cell to determine the weight of filtrate received. The excess slurry was then pumped back into the reservoir tank and, in order to keep a constant slurry concentration, a compensating

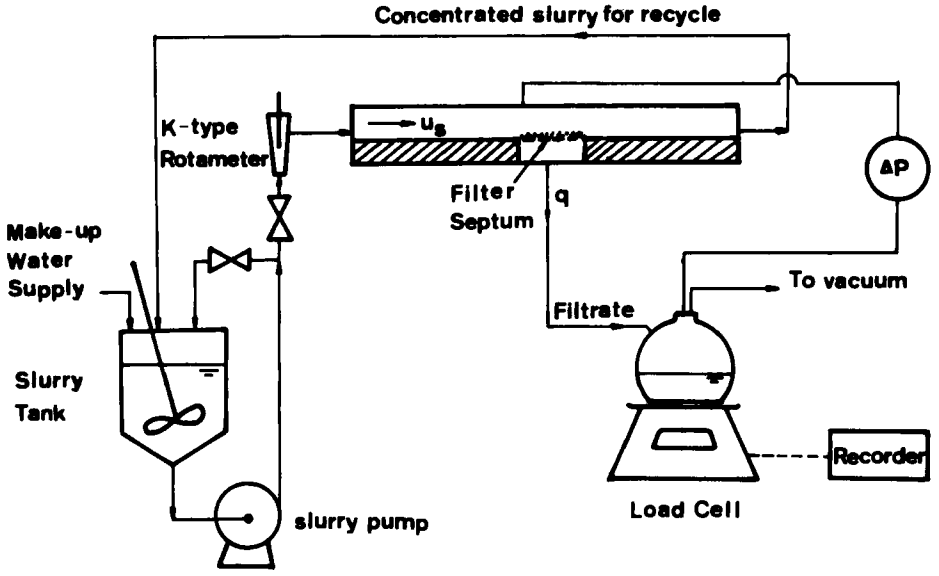

FIG. 3a. A schematic diagram of crossflow filtration.

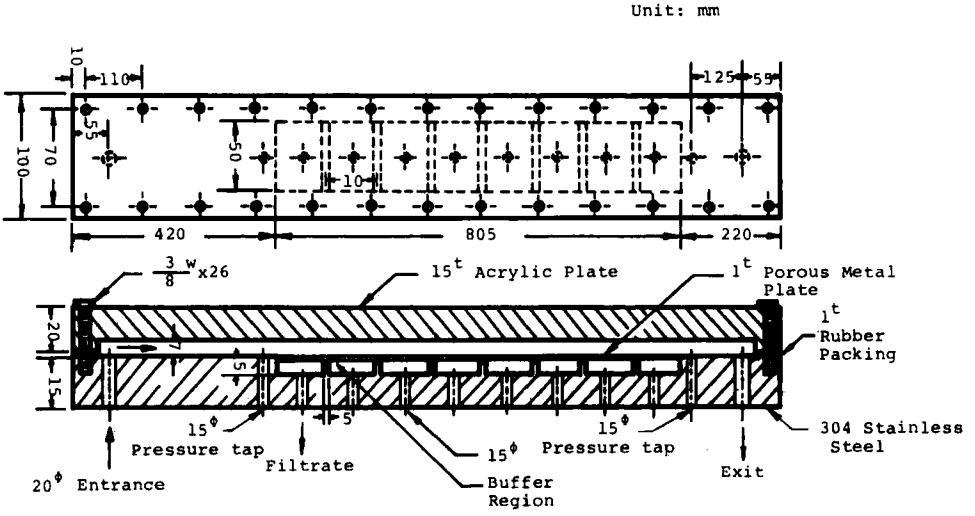

FIG. 3b. A detailed construction of the two-dimensional crossflow filter.

volume of filtrate was continuously added to the tank. By creating a suitable crossflow rate and pressure drop across the filter septum, filtration for enough time to allow a sufficient amount of cake to be deposited on the surface of the filter medium could be controlled. After the filtration was stopped, the very thin layer of deposited particles was carefully scrapped and dispersed in water. The sample was then transferred to the MICROTRAC for particle size distribution analysis.

RESULTS AND DISCUSSIONS

Results

Particle size distributions of cake formed under various filtration rates at 0.86 m/s of crossflow velocity are shown in Fig. 4. This figure shows that all of the particle sizes of cake are less than that of the initial slurry particles, and that a lower filtration rate induces finer deposited particles. These results can explain the results of Lu et al. (*12*) in that finer particles appearing in the upper layer of cake are deposited under a corresponding lower filtration rate.

Since the mass of cake obtained during a very short time of crossflow filtration is too small to measure precisely, the probability function of

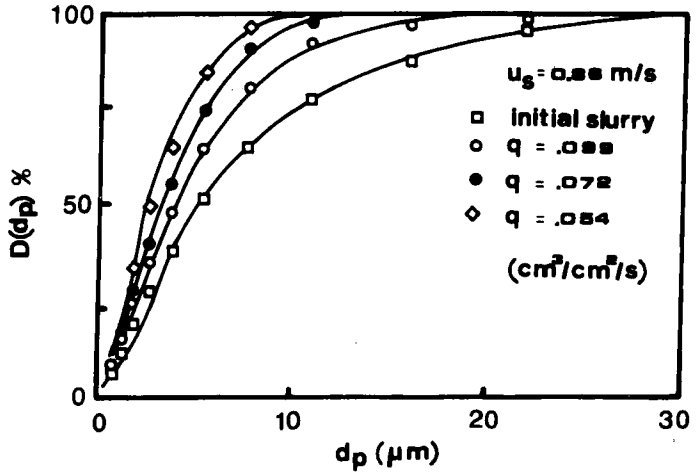

FIG. 4. Undersize particle distribution of cake formed under various filtration rates.

particle deposition $P(d_p)$ calculated from Eq. (22) cannot be obtained directly. However, the tendency of the probability function can be represented by the ratio $f_c(d_p)/f_0(d_p)$ because their values are always proportional to $P(d_p)$ by a constant factor of $c_0\Delta V/\Delta w_c$. Figure 5 shows the typical behavior of the probability function of particle deposition in terms of $f_c(d_p)/f_0(d_p)$ for crossflow filtrations. The almost constant values of $f_c(d_p)/f_0(d_p)$ occurring within a smaller diameter range reveal the existence of a critical selective cut-diameter, even though the probability function curve of particle deposition shows a trailing behavior after the cut-diameter. However, it is very difficult to determine the critical cut-diameter from the probability function curve of particle deposition. If the selective effect on particle deposition is ideal, then by assigning the values of cut-diameter d_{pc}, the theoretical undersize distribution of cake can be calculated by $D_0(d_p)/D_0(d_{pc})$ in order to compare it with the measured particle size distribution of cake to determine the critical cut-diameter by the method of least-square-error curve fitting. Figure 6 compares the results of measurements with the theoretical calculation. From the results of curve fitting, the cut-diameters under various filtration rates q at the slurry velocity u_s = 0.86 m/s are shown in Fig. 7. The figure shows that

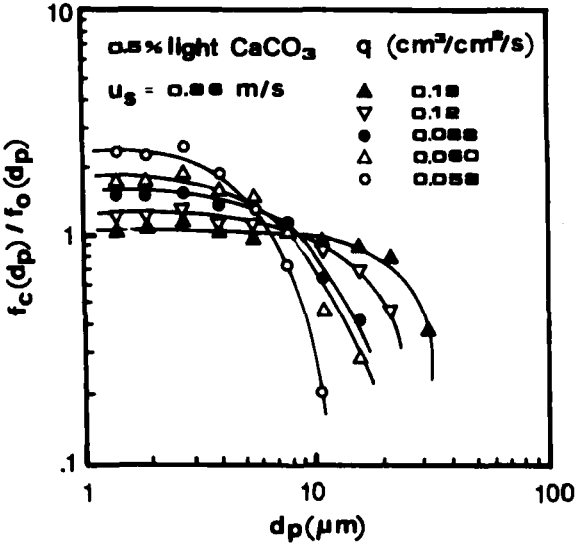

FIG. 5. Probability function of particle deposition expressed by $f_c(d_p)/f_0(d_p)$ under various filtration rates.

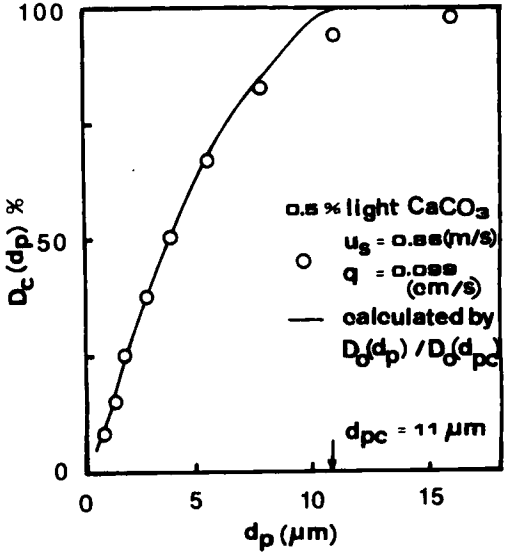

FIG. 6. Comparison of undersize distribution of cake particles calculated by $D_0(d_p)/D_0(d_{pc})$ with experimental data.

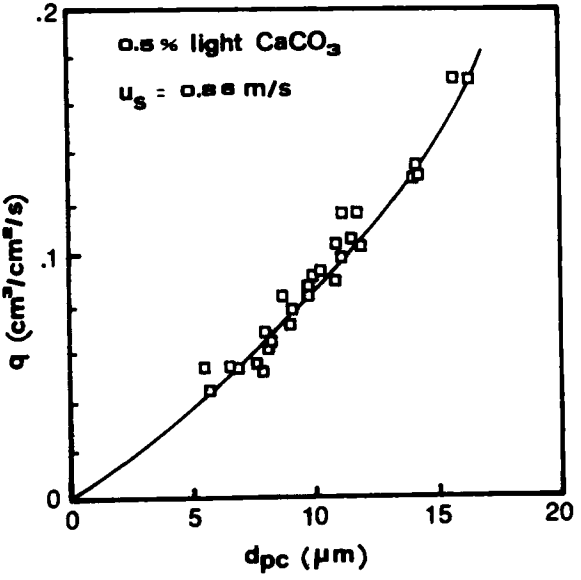

FIG. 7. Dependence of filtration rate and selective cut-diameter in crossflow filtration at u_s = 0.86 m/s.

a decrease in the filtration rate will decrease the size of the deposited particles.

There are two unknown parameters, ϕ and tan θ, in Eq. (18), and they must be determined before the experimental data can be compared with theory. Equation (8) provides a formula to estimate the values of ϕ from the measurement of the resistance of the filter medium, R_m, and the cut-diameter of the deposited particles. R_m, obtained from a constant pressure filtration test of pure water, is different from that obtained by extrapolating the results of a constant pressure filtration test of slurry to time zero. R_m calculated by the latter method was chosen because it is so similar to this filtration system. Ju (*23*) indicated that the resistance of the filter medium determined by the latter method did not always yield the same value even though the same grade of filter medium was used. In order to overcome this uncertainty and simplify the computation, an average value of $\phi = 258$ was calcuated through the whole range of experimental variables under the assumptions of $R_m(\text{ave}) = 2.0 \times 10^8$ 1/cm and $d_{pc}(\text{ave}) = 10$ μm.

The value of the other parameter θ, the angle of repose between particles and the filter medium, is very difficult to determine from an isolated experiment, and its actual physical sense is not only an angle of repose but also a quantitative parameter of all the combined effects of interfacial forces between the particles and the septum surface. Since the viscosity and density of the slurry and the clearance of the filter channel are known, c_2 and c_3 in Eq. (18) can be calculated. From Eq. (17), a plot of $\{q + c_2 d_{pc}^2 - c_3 u_s^{7/2} d_{pc}^3\}$ versus d_{pc} should give a straight line that passes through the origin point and has a slope of $c_1 u_s^{7/4}$. Figure 8 shows a plot of $\{q + c_2 d_{pc}^2 - c_3 u_s^{7/2} d_{pc}^3\}$ versus d_{pc} obtained from the experiment at a crossflow velocity equal to 0.86 m/s. With a slope of 78.3, the straight-line behavior supports our theory. From the slope, a 0.11 value of tan θ is correlated. By applying this result, tan $\theta = 0.11$, the q-u_s-d_{pc} relationship under various crossflow velocities of from 0.57 to 1.14 m/s can be calculated by Eq. (17), and be compared with the experimental data in Fig. 9. The error between experimental measurements and theoretical calculations is within ±30%.

Discussions

I. Resistance of Deposited Cake

Equation (17) predicts that the diameter of deposited particles will gradually decrease due to the decay of filtration flux; therefore, the

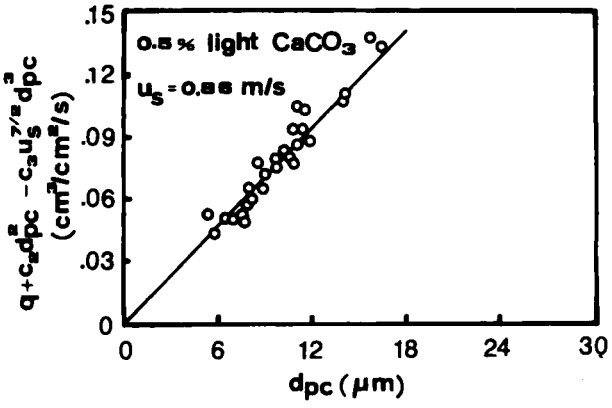

FIG. 8. Plot of $q + c_2 d_{pc}^2 - c_3 u_s^{7/2} d_{pc}^3$ versus d_{pc} at $u_s = 0.86$ m/s.

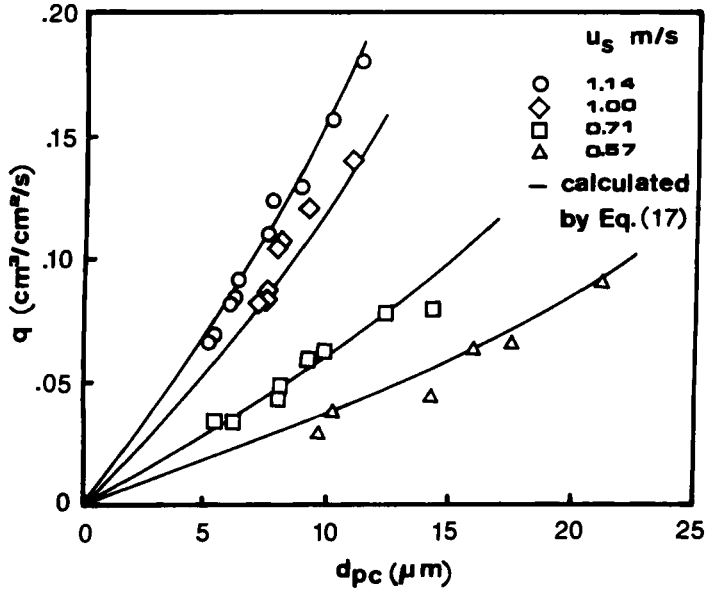

FIG. 9. Comparison of q–d_{pc} relationship calculated from Eq. (17) with experimental data under various crossflow velocities.

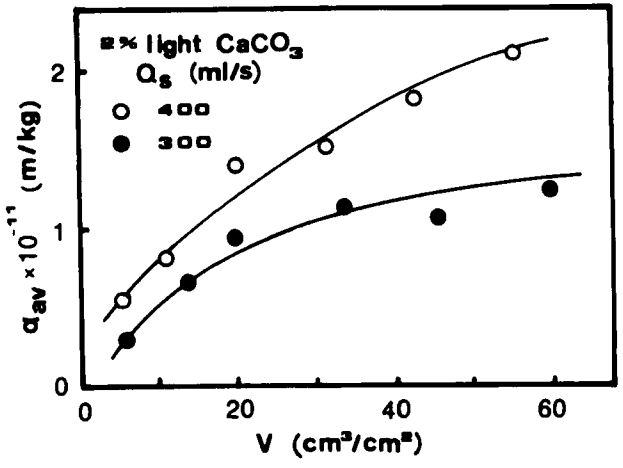

FIG. 10. Increase of average specific resistance of cake during crossflow filtration, 2 wt% of $CaCO_3$ slurry.

deposited particle layer will become finer and finer during crossflow filtration. Grace (*24*) concluded that smaller particles deposited on the cake would give a larger specific resistance to the cake. By measuring the transient filtration rate q and the corresponding deposited cake w_c during constant pressure crossflow filtration, the average specific resistance of cake during crossflow filtration can be calculated by the following equation:

$$q = \frac{\Delta p}{\mu(R_m + \alpha_{av} w_c)} \tag{23}$$

The results are shown in Fig. 10. The increase of average specific resistance of a cake with an increase in the volume of received filtrate implies that smaller sized particles are deposited on the cake.

II. Steady-State Filtration Rate

From the viewpoint of particle deposition, when the filtration rate decays until it is sufficiently small that the corresponding selective cut-diameter of deposited particles is equal to the minimum diameter of slurry particles, then no particles will be supplied from the slurry to

deposit on the septum. In such a case the cake ceases to grow and the system approaches a steady state. By replacing the cut-diameter d_{pc} of Eq. (17) with the minimum diameter of slurry particles, $d_{p,\min}$, the steady-state filtration flux can be predicted to be

$$q_s = c_1 u_s^{7/4} d_{p,\min} - c_2 d_{p,\min}^2 + c_3 u_s^{7/2} d_{p,\min}^3 \tag{24}$$

If the minimum diameter of slurry particles is very small, then the second and third terms on the right-hand side of Eq. (24) can be neglected. By introducing $u_s = Q_s/WH$ into the first term on the right-hand side of Eq. (24), a relationship between the steady-state filtration rate and the cross volumetric flow rate may be obtained:

$$q_s = \frac{0.02609 Q_s^{7/4}}{\phi \tan\theta\, \nu^{3/4} W^{7/4}} \frac{d_{p,\min}}{H^2} \tag{25}$$

In practical operation, one observes that a higher filtration pressure drop forms a greater thickness of cake but gives only a slightly higher steady-state filtration flux. This tendency can be expected from Eq. (25) since the clearance ($H = H_0 - l_c$) of the filter channel is decreased for the case of higher pressure crossflow filtration. Equation (25) also shows that the product of a steady-state flux and the square of the clearance of the filter channel stays constant if the crossflow rate of slurry is unchanged. The experimental data of the steady-state filtration rate under various filtration pressures shown in Table 1 agree with this discussion.

In addition, the microfiltration data of blood, with $d_p = 8.4$ μm and $\mu = 1.2$ cP, published by Porter (*25*) were used to test this theory. By introducing the definition of the shear rate at the septum wall into Eq. (25), either in a laminar or turbulent case, the relationship between filtrate flux and wall shear rate can be derived as

TABLE 1
The Effect of Filtration Pressure Drop on the Steady-State Filtration Rate in Crossflow Filtration (2% light $CaCO_3$, $q_s = 400$ mL/s)

ΔP (cmHg)	q_s (cm/s)	l_c (mm)	H (mm)	$Q_s H^2 \times 10^3$ cm^3/s
25.8	.0200	1.27	5.73	6.6
30.0	.0218	1.38	5.62	6.9
63.3	.0244	1.74	5.26	6.8

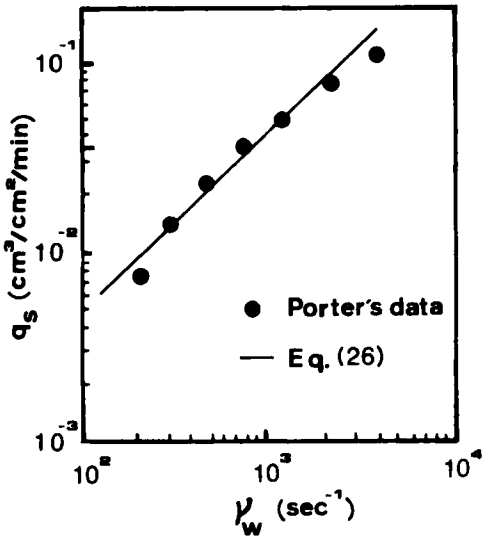

FIG. 11. Comparison of theoretical prediction by Eq. (26) with the experimental microfiltration of blood published by Porter (*25*).

$$q_s = \frac{0.85\gamma_w}{\phi \tan\theta} d_{p,\min} \tag{26}$$

Because the filtrate flux is about 0.05 cm/min at a wall shear rate of 10^3 s^{-1} and the transmembrane pressure drop of filtration is about 10 cmHg, an average ϕ value of 1900 was calculated from Eq. (8). By using $\tan\theta = 0.4$, Eq. (26) shows the correct order of magnitude of the filtrate-flux prediction and the reasonable shear rate dependence shown in Fig. 11.

In a turbulent flow region, and neglecting the decrease in the clearance of the filter channel due to cake formation, Eq. (25) shows that the steady-state filtration rate is proportional to the 1.75 power of the crossflow rate. In practical operation, cake always forms, thereby decreasing the clearance of the filter channel, so the dependence of the crossflow effect on filtration flux will decrease to be less than the 1.75 power. Without any information regarding the cake, it is very difficult to determine the correct dependence of the crossflow rate on filtration flux explicitly.

III. Tractive Conditions of Cake in Laminar Crossflow Filtration

For the case of laminar crossflow filtration, by rearranging Eq. (19):

$$u_s = \frac{1}{c_4 d_{pc}} q + \frac{c_2}{c_4} d_{pc} \tag{27}$$

Equation (27) predicts that the relationship between the sweeping crossflow velocity u_s and filtration rate q is a straight line with a higher slope and a lower intercept when the particles of the bed are finer. This prediction agrees qualitatively with the experimental data of Rushton et al. (*9*).

Fischer and Raasch (*5*) explained from their experimental data that an increase in slurry velocity will decrease the filtration rate by the competition of cake reduction and the specific-resistance increase. Koglin (*26*) indicated that very high shear stress exerted on coagulated particles will break the structure of agglomerated particles, decrease the size of agglomerated particles, and finally result in a more compact cake. Further studies of the shear stress effect on the coagulation of slurry particles may give a reliable explanation of Fischer and Raasch's data. Since more fine particles will deposit on a cake when the crossflow velocity is increased, the cake will show a higher specific resistance to an increase in the value of ϕ in Eq. (25). Thus, a decrease in the filtration rate with an increase of the crossflow velocity may be observed.

CONCLUSIONS

To study the mechanism of particle deposition in crossflow filtration, hydrodynamic forces exerted on a single spherical particle touching the surface of a filter medium are analyzed to derive an expression for the selective critical cut-diameter of deposited particles under various slurry velocities and filtration rates in a crossflow filtration system.

$$q = c_1 u_s^{7/4} d_{pc} - c_2 d_{pc}^2 + c_3 u_s^{7/2} d_{pc}^3 \text{ in a turbulent region}$$

$$q = c_4 u_s d_{pc} - c_2 d_{pc}^2 \text{ in a laminar region}$$

Experimental measurements provide evidence of the existence of a critical cut-diameter of deposited particles in crossflow filtration and agree with theoretical prediction within $\pm 30\%$.

Because the filtration rate decays to be sufficiently small, a corresponding cut-diameter of deposited particles whose diameters are less than the minimum diameter of slurry is reached, and then steady-state is attained.

If the sizes of slurry particles are not affected by the crossflow shear

stress, then this theoretical result shows that the steady-state filtration rate is proportional to the shear rate or shear stress at the septum. By expressing the shear rate at the septum in terms of the crossflow rate, the steady-state filtration rate is proportional to the 1.75 power of the cross volumetric flow rate and the -2 power of the clearance of the filter channel in turbulent crossflow filtration.

NOTATIONS

c_0	proportional factor of Δw_c and $\Delta V \left(= \frac{\rho s_0}{1 - m s_0}\right)$ (kg/m^3)
d_p	diameter of particle (m)
d_{pc}	the largest selective cut-diameter of deposited particles in crossflow filtration (m)
$d_{p,\min}$	minimum diameter of particles in slurry (m)
$D_0(d_p)$	undersize distribution function of particles in slurry.
$D_c(d_p)$	undersize distribution function of particles in cake
f	fanning friction factor
F_f	vertical drag force due to the filtration flow (Nt)
F_l	vertical lift force due to the gradient of crossflow velocity (Nt)
F_t	tangent drag force due to the crossflow velocity (Nt)
F_n	combined vertical force of F_f and F_l (Nt)
F_w	submerged weight force of sphere (Nt)
$f_0(d_p)$	frequency distribution function of particles in slurry
$f_c(d_p)$	frequency distribution function of particles in cake
H_0	initial clearance of crossflow channel (m)
H	clearance of crossflow channel ($H = H_0 - l_c$) (m)
l_c	cake thickness (m)
P	hydrodynamic pressure of fluid (Nt/m^2)
$P(d_p)$	probability function of particles deposition
Q_s	volumetric crossflow rate (m^3/s)
q	filtration rate of filtrate (m^3/s $\cdot$ m^2)
q_s	steady-state filtration rate (m^3/s $\cdot$ m^2)
Re	Reynold's number of bulk flow ($= 2u_s H/\nu$)
R_m	the resistance of filter medium defined by $q = \Delta P/\mu R_m$ (1/m)
m	mass ratio of wet cake to dry cake
m_w^+	mass flux ratio of filtration to bulk flow
u	velocity of fluid in the crossflow direction (m/s)

u_p	velocity of fluid at the position of particle center when particle is absent (m/s)
u_s	average crossflow velocity of slurry (m/s)
u^*	friction velocity at wall (m/s)
u^+	universal dimensionless velocity ($\equiv u/u^*$)
u_m	local velocity of fluid at the outer edge of laminar sublayer (m/s)
v	velocity of fluid in normal direction (m/s)
V	volume of filtrate per unit filtration area (m^3/m^2)
W	width of crossflow filter (m)
w_c	mass of dry cake per unit filtration area (kg/m^2)
z^+	dimensionless distance from the filter wall ($\equiv zu^*/\nu$)
α_{av}	average specific resistance of cake (m/kg)
γ_w	shear rate at wall (1/s)
ϕ	correction factor of Stokes' law
μ	viscosity of fluid ($kg/s \cdot m$)
ν	kinematic viscosity of fluid (m^2/s)
ρ, ρ_s, ρ_p	density of fluid, slurry, and particle, respectively (kg/m^3)
τ_w	shear stress at wall (Nt/m^2)
θ	the angle of repose between particle and filter wall (rad)
δ	thickness of laminar sublayer (m)

Acknowledgment

The authors wish to express their sincere gratitude to the National Science Council of the Republic of China for its financial support.

REFERENCES

1. A. I. Zhevnovatyi, "The Thickening of Suspensions without Cake Formation," *Int. J. Chem. Eng., 4(1)*, 124 (1964).
2. J. A. Dahlheimer, D. G. Thoas, and K. A. Kraus, "Hyperfiltration: Application of Woven Fiber Hoses to Hyperfiltration of Salts and Crossflow Filtrations of Suspended Solids," *Ind. Eng. Chem., Process Des. Dev., 4*, 9 (1970).
3. R. J. Baker, A. G. Fane, C. J. D. Fell, and B. H. Yoo, "Factors Affecting Flux in Crossflow Filtration," *Desalination, 53*, 81 (1985).
4. W. M. Lu, S. C. Ju, and J. C. Chuang, *Study on the Mechanism of Cross-Flow Filtration (I)*, Project Report NSC74-0402-E0002-05, Submitted to National Science Council, September 1987.
5. E. Fischer and J. Raasch, "Cross-Flow Filtration," *Ger. Chem. Eng., 8*, 211 (1985).
6. A. L. Zydney and C. K. Colton, "A Concentration Polarization Model for the Filtrate Flux in Cross-Flow Microfiltration of Particulate Suspensions," *Chem. Eng. Commun., 47*, 1 (1986).

7. R. H. Davis and D. T. Leighton, "Shear-Induced Transport of Particle Layer along a Porous Wall," *Chem. Eng. Sci., 42*(2), 275 (1987).
8. M. Shirato, K. Osasa, and Y. Takaoku, "Critical Tractive Condition of Particulate Beds under Permeation," *Kagaku Kogaku, 34,* 773 (1970).
9. A. Rushton, M. Hosseini, and A. Rushton, "Shear Effects in Cake Formation Mechanism," *Filtr. Sep.,* p. 459 (September/October 1979).
10. F. W. Altena and G. Belfort, "Lateral Migration of Spherical Particles in Porous Flow Channel: Application to Membrane Filtration," *Chem. Eng. Sci., 39*(2), 343 (1983).
11. R. J. Forstrom, K. Bartlet, P. L. Blackshear, and T. Wood, "Formed Elements Deposition onto Filtering Walls," *Trans. Am. Soc. Artif. Intern. Organs, 21,* 602 (1975).
12. W. M. Lu, J. C. Chuang, S. C. Ju, and C. Y. Hwang, *Study on the Mechanism of Rotary Filter Press (II),* Project Report NSC74-0410-E002-09, Submitted to National Science Council, September 1986.
13. E. Fischer and J. Raasch, "Model Tests of the Particle Deposition at the Filter Medium in Cross-Flow Filtration," in *4th World Filtration Congress,* Belgium, 1986, p. 11.11.
14. Y. Hirata and R. Ito, "Velocity Distribution and Prediction of Friction Factor and Pressure Gradient in a Turbulent Porous Tube Flow with Injection or Suction," *J. Chem. Eng. Jpn., 14*(4) 277 (1981).
15. H. Schlichting, *Boundary-Layer Theory,* 7th ed., McGraw-Hill, New York, 1979, Chap. 14.
16. M. E. O'Neill, "A Sphere in Contact with a Plane Wall in a Slow Linear Shear Flow," *Chem. Eng. Sci., 23,* 1293 (1968).
17. S. L. Goren, "The Hydrodynamic Force Resisting the Approach of a Sphere to a Plane Permeable Wall," *J. Colloid Interface Sci., 69*(1), 78 (1979).
18. P. G. Saffman, "On the Motion of Small Spheroidal Particles in a Viscous Liquid," *J. Fluid Mech., 1,* 540 (1956).
19. P. Vasseur and R. G. Cox, "The Lateral Migration of Spherical Particle in Two-Dimensional Shear Flows," *Ibid., 78*(Part 2), 385 (1976).
20. D. B. Simon and S. Saul, *Sediment Transport Technology,* Water Resource, Fort Collins, Colorado, 1977, Chap. 7.
21. T. Mizushina, S. Takeshita, and G. Unno, "Eddy Diffusivity in a Turbulent Pipe Flow with Uniform Fluid Injection and Suction through the Wall," *J. Chem. Eng. Jpn.,8*(3), 127 (1975).
22. R. E. Dean, "Reynolds Number Dependence of Skin Friction and Other Bulk Flow Variables in Two-Dimensional Rectangular Duct Flow," *Trans. ASME, J. Fluid Mech., 100,* 215 (1978).
23. S. C. Ju, "The Analysis of Batchwise Gravitational Filtration," Master's Thesis, National Taiwan University, 1982.
24. H. P. Grace, "Resistance and Compressibility of Filter Cakes," *Chem. Eng. Prog., 49,* 303–318, 367–376 (1953).
25. M. C. Porter, "Ultrafiltration of Colloidal Suspensions," *AIChE Symp. Ser., (120),* 21 (1972).
26. B. Koglin, "Influence of Agglomeration of Filterability of Suspensions," *Ger. Chem. Eng., 8,* 217 (1985).

Received by editor June 3, 1988